

Article

Generation and Characterization of Mid-Infrared Supercontinuum in Bulk YAG Pumped by Femtosecond 1937 nm Pulses from a Regenerative Amplifier

Seyed Ali Rezvani ^{1,*}, Yutaka Nomura ² and Takao Fuji ^{1,2}¹ Toyota Technological Institute, Nagoya 468-8511, Japan² Institute for Molecular Science, Okazaki 444-8585, Japan

* Correspondence: rezvani@toyota-ti.ac.jp; Tel.: +81-52-809-1889

† Current address: 2-12-1 Hisakata, Tempaku-ku, Nagoya 468-8511, Japan.

Received: 23 July 2019; Accepted: 14 August 2019; Published: 18 August 2019



Abstract: We have demonstrated the generation of supercontinuum (SC) pulses in bulk, using femtosecond pulses directly derived from a Tm:YAP regenerative amplifier. The SC spans from 380 nm–4 μm . Such an SC combined with the applied 1937-nm pump pulse can be used in a mid-infrared optical parametric amplifier (MIR-OPA). A full characterization of the phase and stability of the SC provides important insight into the performance of such MIR-OPA systems. Using cross-correlation frequency-resolved optical gating (XFROG), we characterized the properties of the MIR section of the SC that can be used as a seed pulse in an MIR-OPA system. The pulse-to-pulse instability rooted in the intrinsic properties of the self-phase modulation process was observed in the retrieved trace and spectrum of the SC. In addition, the effect of the pump pulse quality was studied on the obtainable SC pulses.

Keywords: solid-state lasers; supercontinuum generation; mid-infrared optical parametric amplifiers

1. Introduction

Supercontinuum generation (SCG) plays a pivotal role in many applications such as white-light interferometry [1], optical coherence tomography [2], frequency comb spectroscopy [3], and dual-comb Fourier transform spectroscopy [4]. Moreover, SCG is the backbone of the optical parametric amplification (OPA). Supercontinuum (SC) pulses are used as seed pulses that are to be amplified in the OPA systems by high energy pump pulses. This nonlinear interaction creates the possibility of generating longer wavelength pulses through the generation of the idler pulses [5–8]. Using OPA systems, the realm of few-cycle pulse generation has fallen into our grasp [9–14], and even attosecond pulse generation systems operating based on OPA have been established [15–17].

Unlike optical parametric generation (OPG) sources, in which the carrier-envelope phase (CEP) is uncorrelated with the CEP of the pump, SC sources inherit the CEP of the applied pump, and if the same source were used to pump both the SCG and OPA, passive CEP stability could be achieved for the idler pulses as a result. One of the most commonly-used SCG methods, specially for OPA applications, is to focus intense laser pulses into a bulk material [18]. SCG in bulk has been used in OPA systems as one of the most prominent seed sources [19–24], because supercontinua generated in bulk media generally exhibit a very well-defined phase and good beam quality, which make them ideal seed sources for OPA systems. Alternatively, ultra-broadband SC can be achieved using optical fibers [25]. The largest bandwidth observed for SC generated in fibers comes at the cost of

introducing considerable instability and spectral modulation, as we showed in our previous work in [26], which may render them inapplicable for OPA applications. Similarly, intrinsic properties of the self-phase modulation (SPM) that manifest in the form of complicated temporal pulse splitting and a modulated spectral profile limit the applicable medium length for the SCG in bulk. For this reason, the spectral broadening achieved by the visible and NIR sources in bulk media has not achieved similar bandwidth boundaries as those of the optical fibers [27–29]. As a result, such SCG systems lack the longer wavelength components necessary for the mid-infrared (MIR) applications such as MIR-OPA. To increase the bandwidth of SC, it is important to study the evolution of the nonlinear effects within the materials. Previous studies have shown that the dispersion of the medium can greatly affect the dynamics of the self-focusing [30]. It has been shown that the self-focusing comes to an end by the pulse splitting effect for SCG systems operating at the normal dispersion regimes [31]. Pumping SCG systems at anomalous regions, on the other hand, would result in the extension of the length of the filament and ultra-broadband achievable spectrum [18,32]. Considerable extension of the IR cut-off limits has been reported in previous literature [33–37]. The choice of the medium for SCG depends on a number of factors, among which the most important ones include the damage threshold, transparency range, the nonlinear refractive index, and the required cut-off limits. Sapphire is considered to be an ideal material pumped by NIR sources such as Ti:sapphire lasers, which would cover the 450–1600-nm range [38–40]. Using calcium fluoride (CaF₂) crystals can help extend the limits of the generated SC into the UV down to 250 nm. The application of CaF₂ comes with the downside of being prone to photo-damage [41], which makes them difficult to maintain. Yttrium aluminum garnet (YAG) has been shown to be one of the best candidates for MIR-SCG, because of its low band-gap and high damage threshold [42,43]. The broad bandwidth of the SC is the result of multiple phenomena, including self-focusing, self-phase modulation, pulse splitting, four-wave mixing, self-steepening, etc. [44–47].

In this work, we generated the supercontinuum in 3 mm of YAG using 1937-nm pulses directly obtained from a regenerative amplifier. The obtained supercontinuum, as a result of pumping in the anomalous dispersion region (where the group velocity dispersion is zero or negative), spanned from 380 nm–4 μm. In order to evaluate the viability of the SC for applications such as MIR-OPA, using a sum-frequency generation cross-correlation frequency-resolved optical gating (SFG-XFROG), we characterized the spectral and temporal properties of the mid-IR portion of the SC. Our findings show that the generated SC contains pulse-to-pulse spectral instabilities. The presence of such instabilities may greatly limit the application of such SC. We also showed that such instabilities are highly dependent on the pump spectral quality and can be minimized by increasing this factor in the system.

2. Experimental Setup

The 1937-nm pump pulses used in our scheme were derived from an updated version of the Tm:YAP regenerative amplifier [48], operating under a 10-kHz repetition rate. Figure 1 depicts the schematic of the experimental setup.

The regenerative amplifier was capable of providing 0.122 mJ of pulse energy with a 360-fs pulse duration after 45 round trips, at a crystal temperature of –20 °C. The regenerative amplifier chamber was purged with nitrogen to reduce the effect of absorption from the water molecules [48,49]. The output pulses of the amplifier were recorded with a resolution of 0.04 nm using a spectrum analyzer (Yokogawa-AQ6375 by Yokogawa Meters & Instruments Corporation, Tokyo, Japan). Figure 2 depicts the obtained spectrum. Using an infrared beamsplitter, 15 μJ of the compressed amplified pulses after 45 round trips were selected and loosely focused into a 3-mm YAG plate to generate the supercontinuum. The residual part of the pump from the beam splitter was focused into a 2-mm BBO crystal (cut at $\theta = 20^\circ$) to generate the second harmonic (SH) with 10% efficiency, which will be used for characterizing the phase of the generated SC later on. The full spectrum of the supercontinuum was collected in its entirety, right after generation, and was sent to be recorded by switching between two spectrum analyzers (Yokogawa-AQ6315 and Yokogawa-AQ6375) and a home-built Fourier transform

spectrometer (liquid nitrogen-cooled InSb photoconductive detector) depending on the wavelength region. The responses from the detectors were corrected, and as can be seen from Figure 3, the limits of the spectrum of the SC expanded into MIR region, reaching 4- μm boundaries.

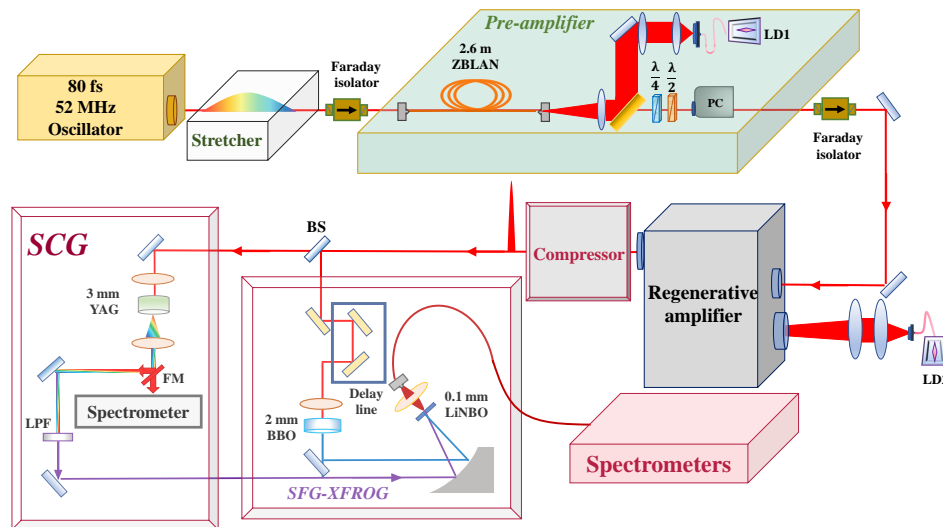


Figure 1. Schematic design of the experimental setup. LD, laser diode. BS, beam splitter. FM, folding mirror. PC, Pockels cell. SCG, supercontinuum generation. SFG-XFROG, sum-frequency generation cross-correlation frequency-resolved optical gating.

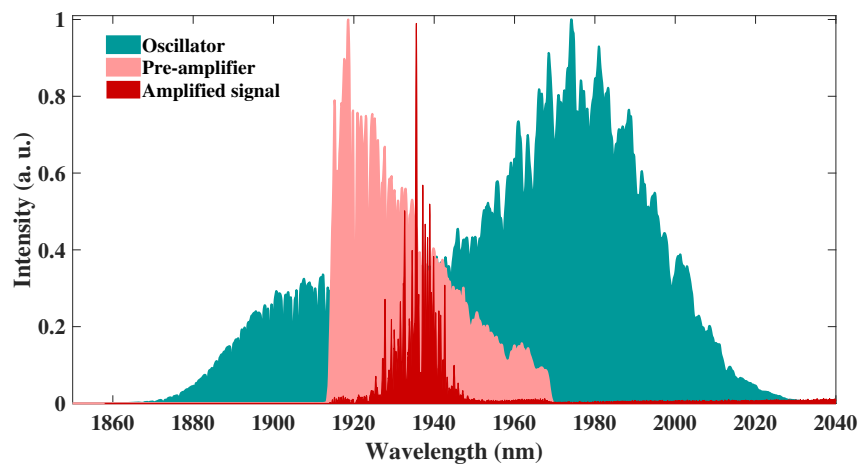


Figure 2. Recorded spectrum of the amplified pulses from the Tm:YAP regenerative amplifier using 23.5 W of absorbed power, operating under 10 kHz and $-20\text{ }^{\circ}\text{C}$.

Detailed knowledge of the phase of the SC plays a pivotal role in applications such as OPA, especially when designing the parameters to maximize OPA systems' performance. For this reason, a pulse characterization system was constructed in our design. The biggest obstacle in characterizing SC pulses arises from the fact that they have in general an ultra-broad bandwidth and very low energy. For this reason, the choice of the characterization system would require adequate considerations. Due to the substantial drawbacks of the second harmonic generation frequency-resolved optical gating method (SHG-FROG) when the subject pulses are too weak to obtain efficient second harmonic signal generation or when the required phase-matching angle for SHG of the pulses would be very large (corresponding to extremely thin non-linear medium), such systems would be rendered inapplicable as the characterization system. While electro-optic sampling schemes have the capability to obtain the properties of the SC pulses, their complexity and technical sophistication would not be deemed suitable for the purpose of our study [50]. XFROG is well known for its capabilities to characterize

complicated pulses [51,52], and since it is based on the nonlinear interaction of a reference pulse, it can be used to measure low energy pulses with a broad bandwidth. Therefore, it was chosen to characterize the SC in our design.

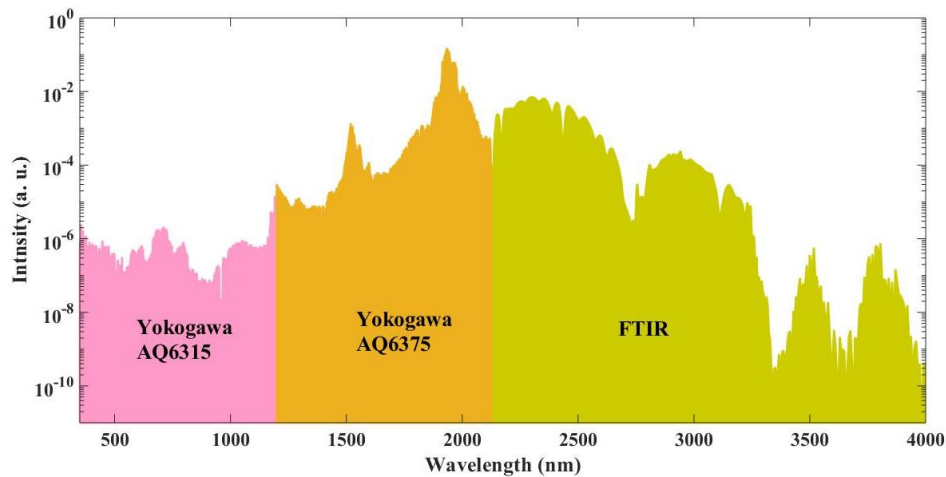


Figure 3. Recorded spectrum of the generated SC in 3-mm YAG.

To characterize a pulse using XFROG, a well-defined reference pulse is required. Although it would be straightforward to use a part of the seed pulse before SC generation as the reference pulse, we chose to use its second harmonic pulse instead because the initial pulse had a very featured spectral profile, and the SH pulses in general exhibited a much cleaner profile. The SH pulses were characterized using a second-harmonic generation FROG (SHG-FROG). The results are summarized in Figure 4. The SHG pulses exhibited a 260-fs pulse duration. Furthermore, the spectral profile was much cleaner, which made it more suitable to be used as the reference for the XFROG. The obtained parameters of the reference pulse from the SHG-FROG were used in the XFROG algorithm. The generated SHG and SC were focused into a 0.1-mm lithium niobate (LiNbO_3) crystal, and the sum-frequency generation (SFG) was achieved. XFROG traces were obtained by measuring the spectra of the SFG beam while changing the delay between the SHG and SC pulses.

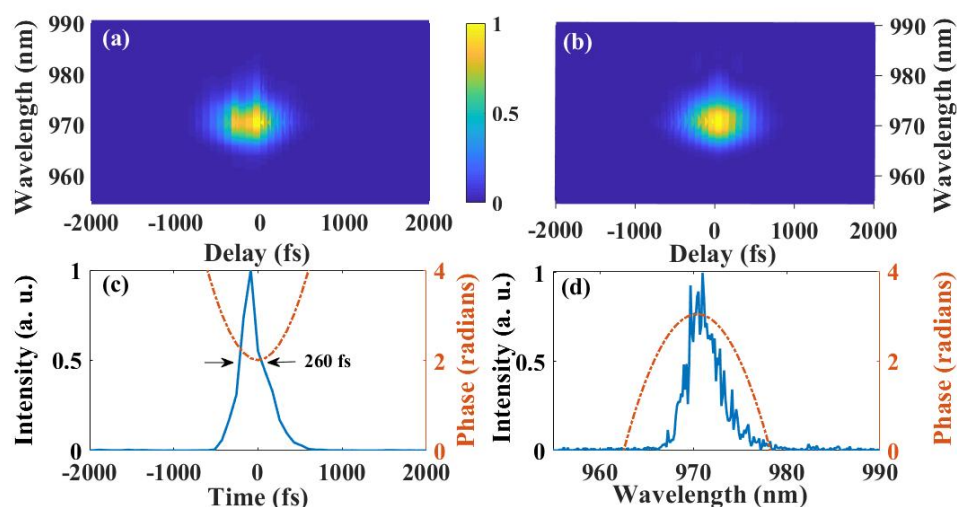


Figure 4. (a) Measured trace, (b) retrieved trace, (c) retrieved temporal profile, and (d) retrieved spectrum from the SHG-FROG with the best error value of 0.004.

3. Results and Discussion

The spectrum of the generated SC obtained by the combination of the spectrum analyzers and the FTIR system is presented in Figure 3. The SC covered 380 nm–4 μ m. Due to the ultra-broad bandwidth of the SC, the main difficulty of its characterization using XFROG arose from the necessary phase-matching angle. Since the MIR portion of the spectrum and their application in MIR-OPA were the main interest of our research, we selected the region above 2.5 μ m using a long pass filter. This indeed lifted the strict requirements on the phase-matching. The properties of this region of the SC were characterized with the SFG-XFROG. The obtained results are presented in Figure 5. As can be seen from Figure 5b,d, the retrieved trace and spectrum exhibited fine features. The discrepancy between the measured trace and the retrieved trace indicated the pulse-to-pulse spectral instability of the generated SC pulses. The fine features could not be detected in the measured trace because each spectrum was accumulated over many shots, and it smeared out such features, making the recorded trace look smooth [53,54]. The information redundancy of the XFROG made it possible for it to recover these features. Indeed, it was shown by Gu et al. that single-shot measurements would reveal similar features in the measured spectrum as well [53].

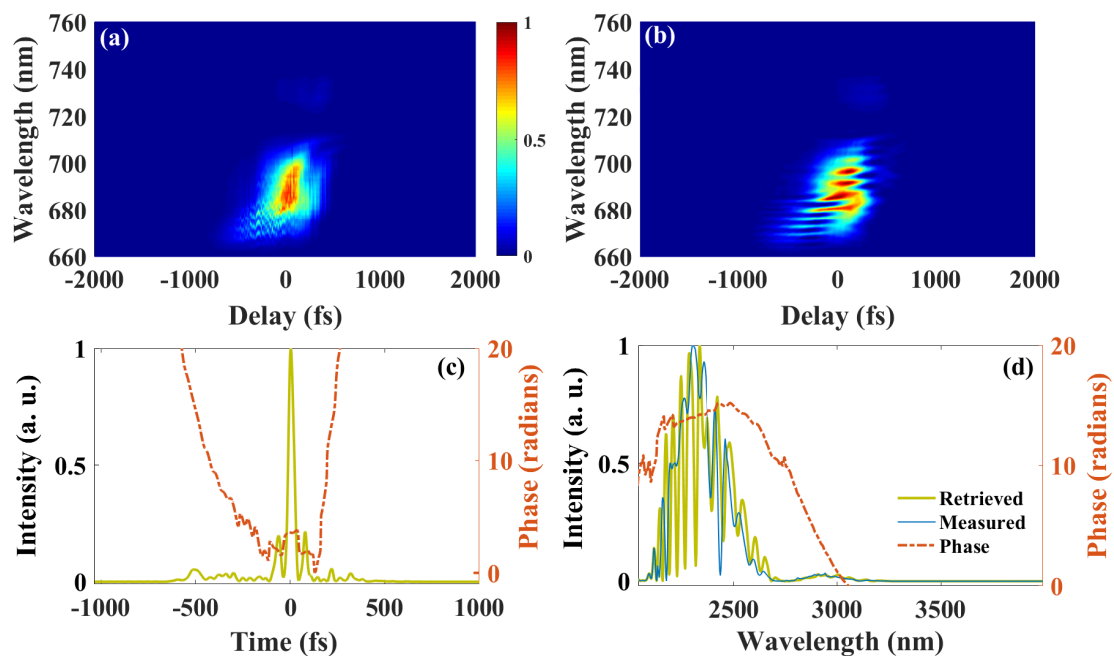


Figure 5. (a) Measured trace, (b) retrieved trace, (c) retrieved temporal profile, and (d) retrieved spectrum from the SFG-XFROG for SC pulses generated by the output of the regenerative amplifier after 45 round trips. Best error value of 0.011.

The spectral phase and stability of the SC from bulk YAG in mid-IR has not been studied so far to the best of our knowledge. Even though the observed instabilities in our results were the intrinsic property of the self-phase modulation process (SPM) in media, the existence of such features may limit the applicability of such SC in fields such as biological applications (e.g., coherent anti-Stokes Raman scattering microscopy) and MIR-OPA systems. Since in the optical parametric amplification process, the amplified signal would inherit seed properties, it is of great importance to minimize the presence of such instabilities in the SC.

It has been previously shown that the SCG process is extremely sensitive to the pump pulse spectral properties [55–57]. Initial instabilities in the pump pulses would result in pulse-to-pulse variation of the SC properties. Due to the fact that the center wavelength of the driving pump in our system fell into the water-absorption region, its spectral profile was highly modulated owing to the water absorption lines, as can be seen in Figure 2. The severity of the spectral modulation was

determined by the propagation distance in air. Since we used a regenerative amplifier to generate the pump pulse, we could control the distance that the pulses traveled in the air by changing the number of round trips that the pulses traveled inside the amplifier cavity. It was previously shown in [48] that reducing the number of the round trips would result in an improved spectral profile and bandwidth of the amplified signal obtained from the regenerative amplifier. We reduced the number of round trips of the initial pump pulses in the regenerative amplifier to two-thirds of the initial value (30 rounds) and re-recorded the spectrum of the output pulses. Figure 6 depicts the comparison between the output spectrum for 45 and 30 round trips (RT). Similar to the previously-reported results in [48], an increase in the bandwidth and improvement on the features inside the spectrum can be observed. Using the same pulse energy (15 μJ), we focused the initial pump pulses from the regenerative amplifier after 30 round trips into the YAG and similarly characterized the generated SC.

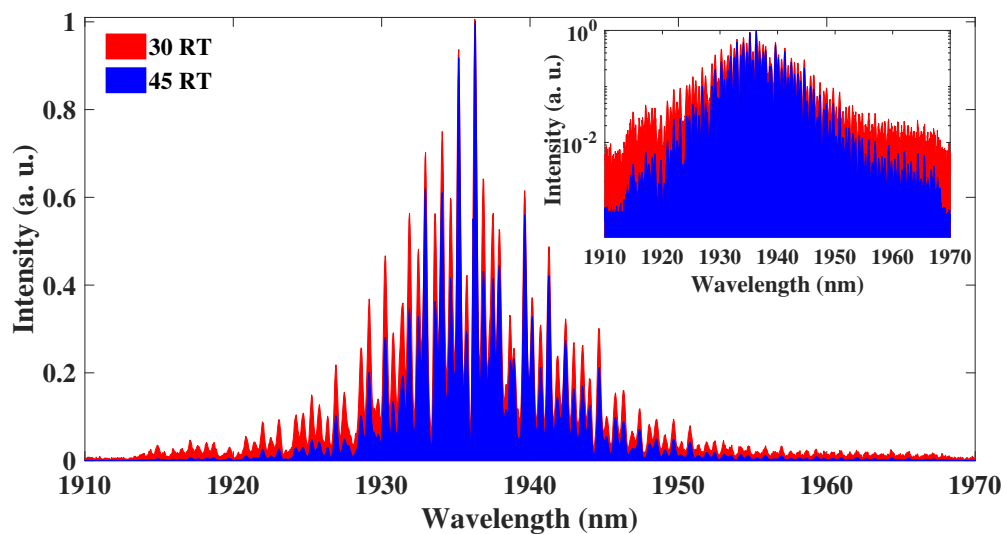


Figure 6. Comparison between the pump pulses after 45 and 30 round trips (RT). Inset: intensity representation in logarithmic scale.

The visible part of the SC spectrum did not exhibit significant changes. Once again, the mid-IR region of the SC, which was of particular interest to us, was recorded using the FTIR system. Figure 7 depicts the results for pump pulses after 30 round trips. The SC spectrum showed obvious signs of improvement at the longer wavelengths with a much smoother profile. We sent the SC to be characterized in the SFG-XFROG, and the results are presented in Figure 8. The retrieved trace and spectrum from the SFG-XFROG in Figure 8b,d exhibited significant improvements and were devoid of the strong modulation observed in Figure 5. The components above 3.5 μm of the SC spectrum were not present in the retrieved spectrum by the XFROG due to the phase-matching bandwidth limitations of the applied non-linear crystal. Such a clean spectral profile combined with the well-defined smooth phase would make the generated supercontinuum a viable candidate for application in MIR-OPA systems. Such systems pumped at the vicinity of 2 μm by a regenerative amplifier and seeded by the SC from YAG hold the promise of achieving MIR pulses with a wavelength as long as 11 μm in the form of the idler in a single stage.

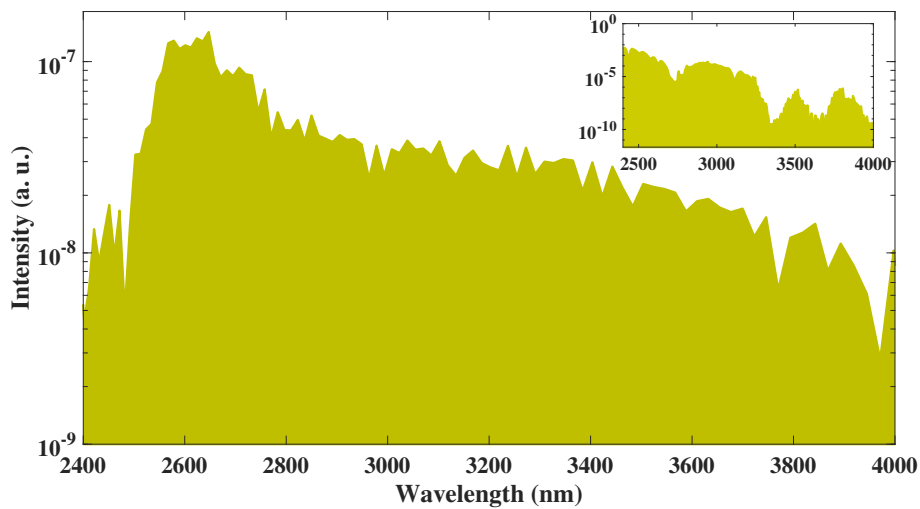


Figure 7. Supercontinuum spectrum using the pump pulses after 30 round trips. Inset: MIR portion of the SC spectrum generated by pump pulses after 45 round trips.

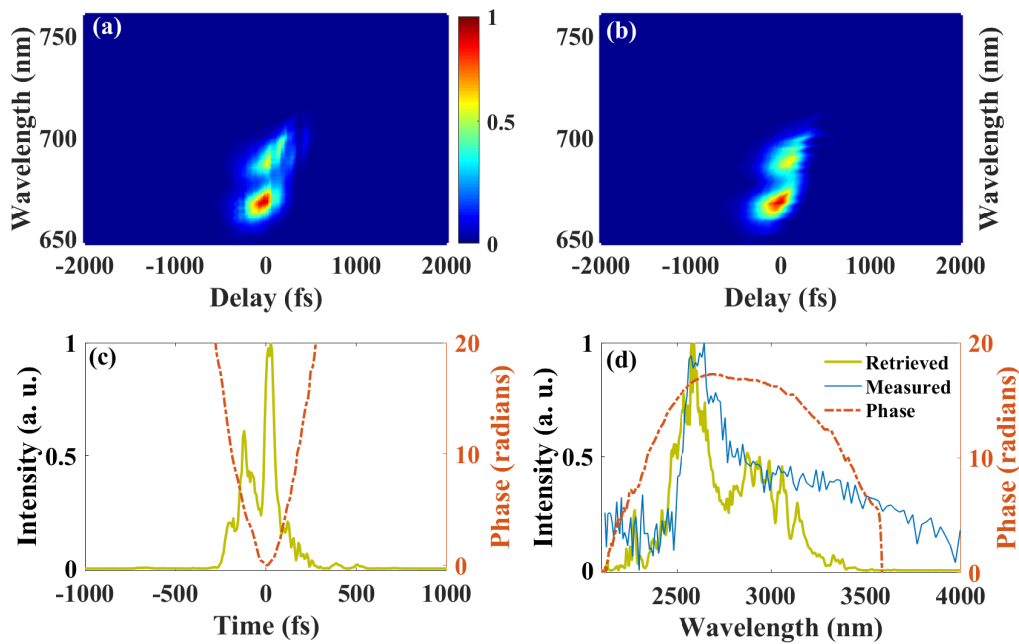


Figure 8. (a) Measured trace, (b) retrieved trace, (c) retrieved temporal profile, and (d) retrieved spectrum from the SFG-XFROG for SC pulses generated by the output of the regenerative amplifier after 30 round trips. Best error value of 0.008.

One drawback of reducing the round trips of the regenerative amplifier is a significant drop in the output energy. In the case of 30 RT, the amplifier was only capable of generating 0.07 mJ. That would hint toward the necessity of adding an additional fiber pre-amplifier to the regenerative amplifier system in order to provide a well-suited pump source for a scalable MIR-OPA design.

4. Conclusions

In this work, we generated the supercontinuum in 3 mm of bulk YAG, using fs pulses directly derived from a thulium-based regenerative amplifier. The boundaries of the generated SC started from 380 nm and reached 4 μm . The mid-infrared portion of such an SC can be a great candidate for seeding the MIR-OPA systems pumped by 1937-nm pulses generated in the regenerative amplifier,

which has the potential to obtain pulses with a wavelength as long as 11 μm . We characterized this portion of the SC with SFG-XFROG and experimentally showed that the SC contained pulse-to-pulse spectral instability. The presence of such modulations limits the applicability of the SC for applications and specifically OPA. Controlling the spectral profile of the pump pulses, we also achieved stable SC pulses that exhibited a clean spectral profile and a smooth phase simultaneously. Having such SC pulses at hand creates the opportunity for a compact and simple MIR-OPA design.

Author Contributions: S.A.R. was in charge of designing the system and writing the manuscript. All the conducted experiments in the manuscript were also conducted by S.A.R. The development of the Tm: fiber oscillator and amplifier and the FROG data analysis was contributed to by Y.N. T.F. contributed to the development of the Tm:YAP laser system and had oversight over the whole project as the head of the group. All authors reviewed the contents of the manuscript and provided comments.

Funding: Core Research for Evolutional Science and Technology (CREST) (JPMJCR17N5).

Conflicts of Interest: The authors declare no conflict of interest.

References

1. Kassamakov, I.; Hanhijärvi, K.; Abbadi, I.; Aaltonen, J.; Ludvigsen, H.; Hægström, E. Scanning white-light interferometry with a supercontinuum source. *Opt. Lett.* **2009**, *34*, 1582–1584. [[CrossRef](#)] [[PubMed](#)]
2. Nishizawa, N.; Kawagoe, H.; Yamanaka, M.; Matsushima, M.; Mori, K.; Kawabe, T. Wavelength Dependence of Ultrahigh-Resolution Optical Coherence Tomography Using Supercontinuum for Biomedical Imaging. *IEEE J. Sel. Top. Quantum Electron.* **2019**, *25*, 1–15. [[CrossRef](#)]
3. Schliesser, A.; Picqué, N.; Hänsch, T.W. Mid-infrared frequency combs. *Nat. Photonics* **2012**, *6*, 440–449. [[CrossRef](#)]
4. Coddington, I.; Newbury, N.; Swann, W. Dual-comb spectroscopy. *Optica* **2016**, *3*, 414–426. [[CrossRef](#)]
5. Rezvani, S.A.; Zhang, Q.; Hong, Z.; Lu, P. Tunable broadband intense IR pulse generation at non-degenerate wavelengths using group delay compensation in a dual-crystal OPA scheme. *Opt. Express* **2016**, *24*, 11187–11198. [[CrossRef](#)] [[PubMed](#)]
6. Zhang, Q.; Takahashi, E.J.; Mücke, O.D.; Lu, P.; Midorikawa, K. Dual-chirped optical parametric amplification for generating few hundred mJ infrared pulses. *Opt. Express* **2011**, *19*, 7190–7212. [[CrossRef](#)] [[PubMed](#)]
7. Mundry, J.; Lohrenz, J.; Betz, M. Tunable femtosecond near-IR source by pumping an OPA directly with a 90 MHz Yb: fiber source. *Appl. Opt.* **2017**, *56*, 3104–3108. [[CrossRef](#)] [[PubMed](#)]
8. Andersen, T.V.; Schmidt, O.; Bruchmann, C.; Limpert, J.; Aguergaray, C.; Cormier, E.; Tünnermann, A. High repetition rate tunable femtosecond pulses and broadband amplification from fiber laser pumped parametric amplifier. *Opt. Express* **2006**, *14*, 4765–4773. [[CrossRef](#)] [[PubMed](#)]
9. Liang, H.; Krogen, P.; Wang, Z.; Park, H.; Kroh, T.; Zawilski, K.; Schunemann, P.; Moses, J.; DiMauro, L.F.; Kärtner, F.X.; et al. High-energy mid-infrared sub-cycle pulse synthesis from a parametric amplifier. *Nat. Commun.* **2017**, *8*, 141. [[CrossRef](#)] [[PubMed](#)]
10. Huang, S.W.; Cirmi, G.; Moses, J.; Hong, K.H.; Bhardwaj, S.; Birge, J.R.; Chen, L.J.; Li, E.; Eggleton, B.J.; Cerullo, G.; et al. High-energy pulse synthesis with sub-cycle waveform control for strong-field physics. *Nat. Photonics* **2011**, *5*, 475–479. [[CrossRef](#)]
11. Yin, Y.; Li, J.; Ren, X.; Wang, Y.; Chew, A.; Chang, Z. High-energy two-cycle pulses at 3.2 μm by a broadband-pumped dual-chirped optical parametric amplification. *Opt. Express* **2016**, *24*, 24989–24998. [[CrossRef](#)] [[PubMed](#)]
12. Ishii, N.; Xia, P.; Kanai, T.; Itatani, J. Optical parametric amplification of carrier-envelope phase-stabilized mid-infrared pulses generated by intra-pulse difference frequency generation. *Opt. Express* **2019**, *27*, 11447–11454. [[CrossRef](#)] [[PubMed](#)]
13. Brida, D.; Cirmi, G.; Manzoni, C.; Bonora, S.; Villorosi, P.; Silvestri, S.D.; Cerullo, G. Sub-two-cycle light pulses at 1.6 μm from an optical parametric amplifier. *Opt. Lett.* **2008**, *33*, 741–743. [[CrossRef](#)] [[PubMed](#)]
14. Hong, Z.; Zhang, Q.; Rezvani, S.A.; Lan, P.; Lu, P. Tunable few-cycle pulses from a dual-chirped optical parametric amplifier pumped by broadband laser. *Opt. Laser Technol.* **2018**, *98*, 169–177. [[CrossRef](#)]
15. Calegari, F.; Sansone, G.; Stagira, S.; Vozzi, C.; Nisoli, M. Advances in attosecond science. *J. Phys. B At. Mol. Opt. Phys.* **2016**, *49*, 062001. [[CrossRef](#)]

16. Chen, M.C.; Mancuso, C.; Hernández-García, C.; Dollar, F.; Galloway, B.; Popmintchev, D.; Huang, P.C.; Walker, B.; Plaja, L.; Jaroń-Becker, A.A.; et al. Generation of bright isolated attosecond soft X-ray pulses driven by multicycle midinfrared lasers. *Proc. Natl. Acad. Sci. USA* **2014**, *111*, E2361–E2367. [[CrossRef](#)] [[PubMed](#)]
17. Takahashi, E.J.; Lan, P.; Mücke, O.D.; Nabekawa, Y.; Midorikawa, K. Infrared Two-Color Multicycle Laser Field Synthesis for Generating an Intense Attosecond Pulse. *Phys. Rev. Lett.* **2010**, *104*, 233901. [[CrossRef](#)] [[PubMed](#)]
18. Silva, F.; Austin, D.R.; Thai, A.; Baudisch, M.; Hemmer, M.; Faccio, D.; Couairon, A.; Biegert, J. Multi-octave supercontinuum generation from mid-infrared filamentation in a bulk crystal. *Nat. Commun.* **2012**, *3*, 807. [[CrossRef](#)] [[PubMed](#)]
19. Manzoni, C.; Cerullo, G. Design criteria for ultrafast optical parametric amplifiers. *J. Opt.* **2016**, *18*, 103501. [[CrossRef](#)]
20. Shirakawa, A.; Sakane, I.; Takasaka, M.; Kobayashi, T. Sub-5-fs visible pulse generation by pulse-front-matched noncollinear optical parametric amplification. *Appl. Phys. Lett.* **1999**, *74*, 2268–2270. [[CrossRef](#)]
21. Brida, D.; Manzoni, C.; Cirmi, G.; Marangoni, M.; Silvestri, S.D.; Cerullo, G. Generation of broadband mid-infrared pulses from an optical parametric amplifier. *Opt. Express* **2007**, *15*, 15035–15040. [[CrossRef](#)] [[PubMed](#)]
22. Zavelani-Rossi, M.; Cerullo, G.; Silvestri, S.D.; Gallmann, L.; Matuschek, N.; Steinmeyer, G.; Keller, U.; Angelow, G.; Scheuer, V.; Tschudi, T. Pulse compression over a 170-THz bandwidth in the visible by use of only chirped mirrors. *Opt. Lett.* **2001**, *26*, 1155–1157. [[CrossRef](#)] [[PubMed](#)]
23. Baltuška, A.; Fuji, T.; Kobayashi, T. Visible pulse compression to 4 fs by optical parametric amplification and programmable dispersion control. *Opt. Lett.* **2002**, *27*, 306–308. [[CrossRef](#)] [[PubMed](#)]
24. Hong, Z.; Rezvani, S.A.; Zhang, Q.; Cao, W.; Lu, P. Ultrabroadband microjoule 1.8 μm laser pulse from a single-stage broadband pumped OPA. *Opt. Lett.* **2018**, *43*, 3706–3709. [[CrossRef](#)] [[PubMed](#)]
25. Qin, G.; Yan, X.; Kito, C.; Liao, M.; Chaudhari, C.; Suzuki, T.; Ohishi, Y. Ultrabroadband supercontinuum generation from ultraviolet to 6.28 μm in a fluoride fiber. *Appl. Phys. Lett.* **2009**, *95*, 161103. [[CrossRef](#)]
26. Rezvani, S.A.; Nomura, Y.; Ogawa, K.; Fuji, T. Generation and characterization of mid-infrared supercontinuum in polarization maintained ZBLAN fibers. *Opt. Express* **2019**, *27*, in press. [[CrossRef](#)]
27. Gaeta, A.L. Catastrophic Collapse of Ultrashort Pulses. *Phys. Rev. Lett.* **2000**, *84*, 3582–3585. [[CrossRef](#)]
28. Fibich, G.; Papanicolaou, G.C. Self-focusing in the presence of small time dispersion and nonparaxiality. *Opt. Lett.* **1997**, *22*, 1379–1381. [[CrossRef](#)]
29. Bradler, M.; Baum, P.; Riedle, E. Femtosecond continuum generation in bulk laser host materials with sub- μm pump pulses. *Appl. Phys. B* **2009**, *97*, 561. [[CrossRef](#)]
30. Luther, G.G.; Moloney, J.V.; Newell, A.C.; Wright, E.M. Self-focusing threshold in normally dispersive media. *Opt. Lett.* **1994**, *19*, 862–864. [[CrossRef](#)]
31. Faccio, D.; Porras, M.A.; Dubietis, A.; Bragheri, F.; Couairon, A.; Di Trapani, P. Conical Emission, Pulse Splitting, and X-Wave Parametric Amplification in Nonlinear Dynamics of Ultrashort Light Pulses. *Phys. Rev. Lett.* **2006**, *96*, 193901. [[CrossRef](#)]
32. Saliminia, A.; Chin, S.L.; Vallée, R. Ultra-broad and coherent white light generation in silica glass by focused femtosecond pulses at 1.5 μm . *Opt. Express* **2005**, *13*, 5731–5738. [[CrossRef](#)]
33. Hemmer, M.; Baudisch, M.; Thai, A.; Couairon, A.; Biegert, J. Self-compression to sub-3-cycle duration of mid-infrared optical pulses in dielectrics. *Opt. Express* **2013**, *21*, 28095–28102. [[CrossRef](#)]
34. Garejev, N.; Tamošauskas, G.; Dubietis, A. Comparative study of multioctave supercontinuum generation in fused silica, YAG, and LiF in the range of anomalous group velocity dispersion. *J. Opt. Soc. Am. B* **2017**, *34*, 88–94. [[CrossRef](#)]
35. Chekalin, S.V.; Kompanets, V.O.; Smetanina, E.O.; Kandidov, V.P. Light bullets and supercontinuum spectrum during femtosecond pulse filamentation under conditions of anomalous group-velocity dispersion in fused silicalicati. *Quantum Electron.* **2013**, *43*, 326–331. [[CrossRef](#)]
36. Durand, M.; Jarnac, A.; Houard, A.; Liu, Y.; Grabielle, S.; Forget, N.; Durécu, A.; Couairon, A.; Mysyrowicz, A. Self-Guided Propagation of Ultrashort Laser Pulses in the Anomalous Dispersion Region of Transparent Solids: A New Regime of Filamentation. *Phys. Rev. Lett.* **2013**, *110*, 115003. [[CrossRef](#)]

37. Dubietis, A.; Tamosauskas, G.; Šūminas, R.; Jukna, V.; Couairon, A. Ultrafast supercontinuum generation in bulk condensed media. *Lith. J. Phys.* **2017**, *57*, 113–157. [[CrossRef](#)]
38. Ashcom, J.B.; Gattass, R.R.; Schaffer, C.B.; Mazur, E. Numerical aperture dependence of damage and supercontinuum generation from femtosecond laser pulses in bulk fused silica. *J. Opt. Soc. Am. B* **2006**, *23*, 2317–2322. [[CrossRef](#)]
39. Rezvani, S.A.; Hong, Z.; Pang, X.; Wu, S.; Zhang, Q.; Lu, P. Ultrabroadband tunable OPA design using a spectrally broadened pump source. *Opt. Lett.* **2017**, *42*, 3367–3370. [[CrossRef](#)]
40. Jukna, V.; Galinis, J.; Tamosauskas, G.; Majus, D.; Dubietis, A. Infrared extension of femtosecond supercontinuum generated by filamentation in solid-state media. *Appl. Phys. B* **2014**, *116*, 477–483. [[CrossRef](#)]
41. Huber, R.; Satzger, H.; Zinth, W.; Wachtveitl, J. Noncollinear optical parametric amplifiers with output parameters improved by the application of a white light continuum generated in CaF₂. *Opt. Commun.* **2001**, *194*, 443–448. [[CrossRef](#)]
42. Galinis, J.; Tamošauskas, G.; Gražulevičiūtė, I.; Keblytė, E.; Jukna, V.; Dubietis, A. Filamentation and supercontinuum generation in solid-state dielectric media with picosecond laser pulses. *Phys. Rev. A* **2015**, *92*, 033857. [[CrossRef](#)]
43. Cheng, S.; Chatterjee, G.; Tellkamp, F.; Ruehl, A.; Miller, R.J.D. Multi-octave supercontinuum generation in YAG pumped by mid-infrared, multi-picosecond pulses. *Opt. Lett.* **2018**, *43*, 4329–4332. [[CrossRef](#)]
44. Alfano, R.R.; Li, Q.X.; Jimbo, T.; Manassah, J.T.; Ho, P.P. Induced spectral broadening of a weak picosecond pulse in glass produced by an intense picosecond pulse. *Opt. Lett.* **1986**, *11*, 626–628. [[CrossRef](#)]
45. Manassah, J.T.; Baldeck, P.L.; Alfano, R.R. Thermal focusing effects on the supercontinuum. *Appl. Opt.* **1988**, *27*, 3586–3587. [[CrossRef](#)]
46. Golub, I. Optical characteristics of the supercontinuum generation. *Opt. Lett.* **1999**, *15*, 305–307. [[CrossRef](#)]
47. Xing, Q.; Yoo, K.M.; Alfano, R.R. Self-bending of light. *Opt. Lett.* **1993**, *18*, 479–481. [[CrossRef](#)]
48. Rezvani, S.A.; Suzuki, M.; Malevich, P.; Livache, C.; de Montgolfier, J.V.; Nomura, Y.; Tsurumachi, N.; Baltuška, A.; Fuji, T. Millijoule femtosecond pulses at 1937 nm from a diode-pumped ring cavity Tm:YAP regenerative amplifier. *Opt. Express* **2018**, *26*, 29460–29470. [[CrossRef](#)]
49. Wienke, A.; Wandt, D.; Morgner, U.; Neumann, J.; Kracht, D. 700 MW peak power of a 380 fs regenerative amplifier with Tm:YAP. *Opt. Express* **2015**, *23*, 16884–16889. [[CrossRef](#)]
50. Keiber, S.; Sederberg, S.; Schwarz, A.; Trubetskov, M.; Pervak, V.; Krausz, F.; Karpowicz, N. Electro-optic sampling of near-infrared waveforms. *Nat. Photonics* **2016**, *10*, 159–162. [[CrossRef](#)]
51. DeLong, K.W.; Trebino, R.; Hunter, J.; White, W.E. Frequency-resolved optical gating with the use of second-harmonic generation. *J. Opt. Soc. Am. B* **1994**, *11*, 2206–2215. [[CrossRef](#)]
52. Trebino, R.; Dudley, J.; Gu, X. Ultrafast Technology: Measuring and Understanding the Most Complex Ultrashort Pulse Ever Generated. *Opt. Photonics News* **2003**, *14*, 44. [[CrossRef](#)]
53. Gu, X.; Xu, L.; Kimmel, M.; Zeek, E.; O’Shea, P.; Shreenath, A.P.; Trebino, R.; Windeler, R.S. Frequency-resolved optical gating and single-shot spectral measurements reveal fine structure in microstructure-fiber continuum. *Opt. Lett.* **2002**, *27*, 1174–1176. [[CrossRef](#)]
54. Dudley, J.M.; Gu, X.; Xu, L.; Kimmel, M.; Zeek, E.; O’Shea, P.; Trebino, R.; Coen, S.; Windeler, R.S. Cross-correlation frequency resolved optical gating analysis of broadband continuum generation in photonic crystal fiber: Simulations and experiments. *Opt. Express* **2002**, *10*, 1215–1221. [[CrossRef](#)]
55. Sørensen, S.T.; Larsen, C.; Møller, U.; Moselund, P.M.; Thomsen, C.L.; Bang, O. Influence of pump power and modulation instability gain spectrum on seeded supercontinuum and rogue wave generation. *J. Opt. Soc. Am. B* **2012**, *29*, 2875–2885. [[CrossRef](#)]
56. Henry, C.H.; Kazarinov, R.F. Quantum noise in photonics. *Rev. Mod. Phys.* **1996**, *68*, 801–853. [[CrossRef](#)]
57. Vanholsbeeck, F.; Martin-Lopez, S.; González-Herráez, M.; Coen, S. The role of pump incoherence in continuous-wave supercontinuum generation. *Opt. Express* **2005**, *13*, 6615–6625. [[CrossRef](#)]

